THE GEOLOGICAL SOCIETY OF AMERICA

BULLETIN

ISSN 0016-7606 VOLUME 114 NUMBER 5 MAY 2002

IN THIS ISSUE:

Cosmogenic radionuclide dating of moraines in northern Pakistan defines glaciations

Timing of multiple late Quaternary glaciations in the Hunza Valley, Karakoram Mountains, northern Pakistan: Defined by cosmogenic radionuclide dating of moraines

Lewis A. Owen*
Department of Earth Sciences, University of California, Riverside, California 92521-0423, USA

Robert C. Finkel
Marc W. Caffee†
Center for Accelerator Mass Spectrometry, Lawrence Livermore National Laboratory, Livermore, California 94550, USA

Lyn Gualtieri
Quaternary Research Center, Box 351360, University of Washington, Seattle, Washington 98195-1360, USA

ABSTRACT

Moraines and associated landforms in the upper Hunza Valley, Karakoram Mountains, northern Pakistan, provide an excellent record of multiple glaciations. During the late Quaternary, glaciers advanced at least eight times. By using ^{10}Be and ^{26}Al surface-exposure dating on moraine boulders and scoured bedrock, we determined the timing of glaciation for four of these glacial advances: ca. 54.7–43.2 ka (Borit Jheel glacial stage), ca. 25.7–21.8 ka (Ghulkin I glacial stage), ca. 18.4–15.3 ka (Ghulkin II glacial stage), and ca. 10.8–9.0 ka (Batura glacial stage). For two of the older advances, the Yunz and Shanoz glacial stages, our data set a limit of >60 ka. Although, at present, the uncertainties in dating make it impossible to describe unequivocally the climate processes controlling glaciations in the Hunza Valley, the results suggest that precipitation changes related to oscillations in the southwest Asian monsoonal system combine with cooling that is broadly associated with Heinrich events to cause glacial advances in this region.

Keywords: cosmogenic radionuclide dating, glaciation, Hunza Valley, Karakoram Mountains, southwest Asian summer monsoon.

INTRODUCTION

The geologic archive attests to numerous changes in climate (Bradley, 1999; Lowe and Walker, 1997). Global climate can be read in marine sediments and polar ice cores (Bradley, 1999; Lowe and Walker, 1997). Regional climate changes are evidenced in many forms. In mountain areas, these changes are recorded in spectacular glacial landforms, such as moraines and valley fills.

Understanding the coupling between regional climate events and global forcing is important because it can yield information on how the climate system works. In addition, the effects of climate change on human populations are related to regional climate events, not to globally averaged forcing. Given the likelihood of future global climate change, exploration of the coupling in past climate changes is of great importance.

A regional climate system of particular interest is the southwest Asian summer monsoon. The precipitation brought by the southwest Asian summer monsoon waters a region of central Asia that directly affects the livelihood of >25% of the world's population (Benn and Owen, 1998). The existence of the monsoon is intimately related to the uplift of the Tibetan plateau and greatly influences the climate in this elevated region (Ruddiman and Kutzbach, 1990; Raymo and Ruddiman, 1992). However, it is not evident whether the monsoon, through its control on the moisture flux, is the primary agent regulating glaciation on the plateau and in its bordering mountain ranges.

The moraine successions in the glaciated valleys along the entire length of the Trans-Himalayan mountain belt record changes of moisture and temperature, and therefore monsoon variability, for at least the last two glacial cycles. Earlier studies suggested that glaciations may have been asynchronous in different parts of the Himalaya and with global glaciations (Benn and Owen, 1998).

To investigate the climate factors at work during the late Quaternary in the mountainous region bordering the Tibetan plateau, we have dated several glacial successions in the Karakoram Mountains, situated in Pakistan at the western end of the Trans-Himalayan mountain belt. The Karakoram range, one of the highest on Earth, has been uplifted to between 7000 and 8000 masl (meters above sea level) by the collision of the Indian and Eurasian plates (cf. Searle, 1991). The rapid uplift (»0.1 mm·yr^{-1}) and intense denudation (Searle, 1991) of this range produced thick Quaternary valley fills and impressive successions of moraines and glacially eroded landforms in this region (Derbyshire et al., 1984; Owen, 1989; Owen and Derbyshire, 1993; Shroder et al., 1989, 1993).

Despite the excellent potential to reconstruct the nature of late Quaternary climate change from the glacial geologic evidence, little research has been undertaken in this region (Derbyshire et al., 1984; Owen, 1988, 1989; Shroder et al., 1989, 1993; Scott, 1992). This

*E-mail: lewis.owen@ucr.edu.
†Present address: Department of Physics/PRIME Lab, Purdue University, 1396 Physics Building, West Lafayette, Indiana 47907-1396, USA.

GSA Bulletin; May 2002; v. 114; no. 5; p. 593-604; 7 figures; 2 tables.

paucity of research is partly due to difficulties of access, both physical and political, and partly due to failure to recognize the potential importance of Himalayan glacial systems for the study of global change. These difficulties have been compounded by the absence of geochronological control. During recent years, however, cosmogenic radionuclide surface-exposure dating has come to provide a new and productive method to date glacial landforms in glaciated high-mountain and semiarid environments (Nishiizumi et al., 1993; Gosse et al., 1995a, 1995b; Phillips et al., 1996, 2000; Sloan et al., 1998; Owen et al., 2001). We have therefore mapped and dated glacial landforms and sediments in the Karakoram Mountains to provide evidence for the episodic advance and retreat of glaciers during the Quaternary and to allow reconstruction of local climate oscillations and rates of glacial erosion and sedimentation. Our reconstruction of the extent and timing of each glaciation has then been used to test the synchronicity of regional and global climate changes. In addition, these results allow a test of whether each glaciation in this region can be correlated with the intensity of the southwest Asian summer monsoon.

RATIONALE

The upper Hunza Valley was chosen for this study because it contains a well-preserved and very detailed record of multiple glaciations in the Karakoram Mountains (Derbyshire and Owen, 1997) (Figs. 1, 2, and 3). The first comprehensive study of the Hunza Valley was undertaken by Derbyshire et al. (1984), who concentrated on the area between the Batura and Ghulkin glaciers (Fig. 1). Subsequent work on the Quaternary glaciations in the Karakoram Mountains and adjacent Himalaya used the chronology of Derbyshire et al. (1984) as a framework (e.g., Owen, 1988, 1989; Shroder et al., 1989, 1993; Scott, 1992). On the basis of landforms and sediments, Derbyshire et al. (1984) identified eight glacial stages (Table 1), each of varying magnitude, and presented four thermoluminescence (TL) and two radiocarbon dates to help define the timing of these glacial cycles (Table 1). However, several of the dates were from locations ~50 km down valley from the Ghulkin-Batura area, and morphostratigraphic correlations across such a distance can be misleading (cf. Owen et al., 1997). Given the exceptionally complete geologic record in this region, our study concentrated on providing a comprehensive set of cosmogenic radionuclide dates to define directly the timing of glaciations in the region between the Ghulkin and Batura glaciers.

GEOMORPHIC CONTEXT FOR COSMOGENIC RADIONUCLIDE DATING

The glaciers in the Hunza Valley have high-altitude source areas (>4500 masl) with annual precipitation totals of >2000 mm. Their snouts extend into the semiarid valley floors (~2700 masl) where the annual precipitation totals <200 mm·yr $^{-1}$ and summer temperatures are frequently >25 °C (Goudie et al., 1984). The glaciers are several hundred meters thick and >5 km long; the Batura Glacier exceeds 50 km in length. These glaciers are also among the steepest in the world (Ghulkin Glacier—8.1°; Pasu Glacier—6.0°; Batura Glacier—2.4°). The Hunza Valley glaciers are classified as high-activity glaciers (Andrews, 1975), as evidenced by considerable snowfall in upper regions and high ablation rates in lower regions. The flow rate for these glaciers is relatively fast: 520–1000 m·yr $^{-1}$ for the Batura Glacier (Batura Glacier Investigation Group, 1979; Shi and Zhang, 1984) and 160 m·yr $^{-1}$ for the Pasu Glacier (Pillewizer, 1957).

The steep and long valley slopes adjacent to the glaciers are important in delivering large quantities of snow and rock to glacier surfaces. Large blocks of rock that fall onto the glacier during avalanches disintegrate easily (cf. Hewitt, 1988), exposing fresh rock surfaces. This supraglacial debris is then transported rapidly toward the glacier snout where the debris is deposited to form high (»100 m) latero-frontal moraines (Fig. 4; Owen and Derbyshire, 1989; Owen, 1994) that continue to build up until the glacier retreats.

Two conditions must be met if cosmogenic radionuclide concentrations in moraine boulders are to be used to determine the age of the moraine. First, the inventory of cosmogenic radionuclides inherited from exposure of the boulder prior to its being incorporated into the moraine must be small. Complex exposure histories can occur in outcrop, prior to the boulder's being incorporated in the flowing ice stream or during an intermediate stage while the boulder was part of an older moraine. There are several factors that mitigate against any importance for inheritance of complex exposure histories in the Hunza Valley moraines: (a) Most of the boulders composing the moraines have been severely abraded during glacial transport (Scott, 1992) or were broken apart by mass-movement processes when they were first entrained in the ice. (b) The high activity of glaciers in the Hunza Valley leads to high rates of sediment transport and deposition that accelerate the rate of glacial erosion. Collins (1998) estimated that rates of abrasion beneath the Batura Glacier are between 3.4 and 4.2 mm·yr $^{-1}$. These high erosion rates help ensure that boulders and bedrock surfaces are deeply eroded and thus reduce the likelihood of significant cosmogenic radionuclide buildup during exposure in outcrop. (c) The fresh surfaces exposed by boulder breakup also reduce the likelihood that inherited cosmogenic radionuclides will be present.

The second condition involves the possibility that a boulder has an exposure age greater than the age of formation of the moraine from which the boulder is sampled. Boulders can contain inherited cosmogenic radionuclides if the boulders have been reworked from older deposits. With each successive glaciation, the advancing glaciers may override previous glacial deposits. Some of the older glacial debris may then be reworked and deposited within the younger moraines. Younger moraines may also lie stratigraphically lower than older moraines if the younger moraines are inset. In this case, colluvial processes may transport older material onto the younger surface. Both cases, therefore, contain the potential that the exposure age of a boulder is greater than that of the moraine from which the boulder was collected.

To account for all of these possibilities, we have collected multiple samples from each moraine. Concordance between ages for several boulders from the same moraine increases the confidence with which the measured cosmogenic radionuclide content can be interpreted to indicate the exposure age of the moraine helps samples that may have had complex exposure histories. Except as noted, the finding of concordance leads us to conclude that for most of our sites we can be confident that the boulder-exposure ages represent the age of the moraine.

An important issue is the relative timing between moraine deposition and glacial advance and retreat. Moraines, in general, continue to be reworked as long as the glacier is advancing and become stabilized only when they are abandoned as the glacier retreats. Because climatic variability is relatively rapid (decadal to millennial time scales), previous workers have assumed that the construction of moraines occurs over a relatively short period and that cosmogenic radionuclide ages for boulders on moraine crests should provide reliable dates on the timing and duration of each glaciation (Gosse et al., 1995a, 1995b; Phillips et al., 1996, 2000). We follow this interpretation and consider that the age of a moraine is a good approximation for the timing of a glacial advance. However, we cannot specify whether the ages represent the time at which maximum glacial extent was reached or the time at which glacial retreat began, or whether the ages bracket the full interval of maximum glacial extent.

METHODS

Field Methods

Field work was undertaken between the Ghulkin and Batura Glaciers in the upper Hunza Valley (Fig. 1). The morphostratigraphic relationships between landforms of different glacial stages were examined together with the surface weathering characteristics of the moraines. Our field observations are consistent with those of Derbyshire et al. (1984) and Li Jijun et al. (1984) for all the landforms sampled. We have accordingly adopted their nomenclature for this study.

Samples were collected on those moraines that could be clearly distinguished and assigned to a particular glacial stage. Three samples, KK98–55, KK98–56, and KK98–57, were collected from a striated bedrock surface. Field observations by Derbyshire et al. (1984) and ourselves led to the conclusion that the Pasu I and Pasu II glacial stages are only hundreds of years old. These surfaces were not sampled. Most of the boulders sampled were quartz-rich leucogranites. The sampled boulders, typically of >1 m diameter, were on moraine crests or on glacially eroded bedrock. On moraine crests, care was taken to sample boulders that ‘‘stood proud’’ (>70 cm in height) and were partly buried. Such boulders are not likely to have toppled or to have had sediment cover for a significant amount of time since they were deposited. The location of each sample was recorded by using a handheld Global Positioning System device, and the local site conditions were noted. These included the possibility of shielding from surrounding mountain slopes, any evidence of erosion that might have produced recent exhumation of boulders, and any evidence of deep weathering of boulders and bedrock (Fig. 1C and Table 2).

Cosmogenic Radionuclide Dating

Clean quartz was separated from these rocks by using a chemical-isolation method (Kohl and Nishiizumi, 1992). The quartz was dissolved in HF and HNO_3. Al concentrations were determined either by atomic absorption spectrometry or by ICP-MS (inductively coupled plasma–mass spectrometry). A Be carrier and an Al carrier were added as needed. Be and Al were separated by anion- and cation-exchange ion chromatography in a chloride medium and purified by reprecipitation of the hydroxides. ^{10}Be ($t_{1/2}$ = 1.5 Ma) and ^{26}Al ($t_{1/2}$ = 0.705 Ma) accelerator mass spectrometry (AMS) measurements were carried out at the Lawrence Livermore National Laboratory AMS facility (Davis et al., 1990). The observed ratios were normalized to ICN ^{10}Be and National Institute of Science and Technology ^{26}Al standards that were diluted by K. Nishiizumi (personal commun., 1995).

The total production rate of ^{10}Be or ^{26}Al at the Earth's surface can be modeled by using equation 1 (Stone et al., 1998b; Granger and Smith, 2000):

$$\begin{aligned} N_i(z) = {} & \{P_{n,i}/[(1/\tau_i) + (\rho\epsilon/\Lambda_n)]\} \\ & \times (1 - e^{-(1/\tau_i + \rho\epsilon/\Lambda_n)t}) \\ & + \{Y_i A_1/[(1/\tau_i) + (\rho\epsilon/L_1)]\} \\ & \times (1 - e^{-(1/\tau_i + \rho\epsilon/L_1)t}) \\ & + \{Y_i A_2/[(1/\tau_i) + (\rho\epsilon/L_2)]\} \\ & \times (1 - e^{-(1/\tau_i + \rho\epsilon/L_2)t}). \end{aligned} \tag{1}$$

In the case of no erosion, equation 1 simplifies to

$$\begin{aligned} N_i(z) = {} & \{(P_{n,i}\tau_1) + (Y_i A_1 + Y_i A_2)\tau_i\} \\ & \times (1 - e^{-t/\tau_i}). \end{aligned} \tag{2}$$

The first line of equation 1 refers to production by secondary-neutron spallation. The second and third lines refer to production by stopped muons. The subscript i equals 10 or 26 and denotes either ^{10}Be or ^{26}Al, $P_{n,i}$ denotes production by neutron spallation at the surface, τ_i is the radioactive mean life (τ_{26} = 1.02 m.y.; τ_{10} = 2.16 m.y.), ε is the rock erosion rate, ρ is density, and Λ_n is the penetration depth for production by neutron spallation (Λ_n = 160 ± 10 g·cm^{-2} (Brown et al., 1992)). Values for the muon-related parameters Y_i, A_1, A_2, L_1, and L_2 are given in Granger et al. (2001). ^{10}Be and ^{26}Al are also produced by fast muons. Production via this mechanism is negligible in all but the most rapidly eroding samples. At sea level and high latitudes, spallation accounts for ~97% of the ^{10}Be and ^{26}Al production at the surface of a rock; negative-muon capture and fast-muon reactions are responsible for only ~3% (Heisinger, 1998; Heisinger and Nolte, 2000).

$P_{n,i}$ in equations 1 and 2 depends on altitude and latitude (Lal and Peters, 1967; Lal, 1991) owing to atmospheric and geomagnetic shielding. Production rates are usually quoted at sea level and high latitude (SLHL) because such scaled values are independent of the geomagnetic-field intensity. Spallogenic production rates can be scaled from SLHL reference values to sample altitude and geographic latitude by using Table 2 of Lal (1991). Dunai (2000) has reevaluated latitude and altitude scaling factors to take into account nondipole components in the geomagnetic field and deviations from the accepted pressure versus altitude relationship for the atmosphere. Use of Dunai's scaling factors yields present-day cosmogenic radionuclide production rates that are ~5% greater at our Hunza Valley sites than those calculated from Lal (1991). Because the correction is small and because it is not yet clear how to deal with the time variation of Dunai's correction factors, we have continued to use the scaling factors from Lal (1991). Production by stopped muons has been scaled for elevation by using an atmospheric attenuation length of 247 g·cm^{-2} and for latitude by assuming the same sea-level variation for stopped muons as for neutrons (Stone et al., 1996). The relative importance of muon production decreases to <1.5% at the 2500–3300 m exposure elevation of the surfaces dated in this paper.

Production rates at latitudes higher than ~60° are independent of the geomagnetic field. At lower-latitude locations, such as the Hunza Valley site at ~36°N, the geomagnetic dipole field varies, producing long-term changes in the production rate. Over the past 60 ka, the geomagnetic-field intensity has fluctuated by almost a factor of four (Guyodo and Valet, 1996). The effect of this change on radionuclide production can be expressed in terms of an equivalent change in geomagnetic latitude. A decrease in field intensity is equivalent to an increase in geomagnetic latitude and vice versa. This relationship is expressed by equation 3 from Nishiizumi et al. (1989):

$$\cos(\lambda_{eff}) = (M_t/M_0)^{1/4}\cos(\lambda_0), \tag{3}$$

where λ_{eff} is the effective geomagnetic latitude for the changed field intensity, M_t is the geomagnetic-field intensity at t, M_0 is the current field intensity, and λ_0 is the current geomagnetic latitude. We have used the Sint200 intensity record of Guyodo and Valet (1996) to calculate effective geomagnetic latitudes according to equation 3. Radionuclide decay has been accounted for by weighting the effective geomagnetic latitudes by $e^{-t/\tau}$, with τ being the nuclide mean life. The field intensity

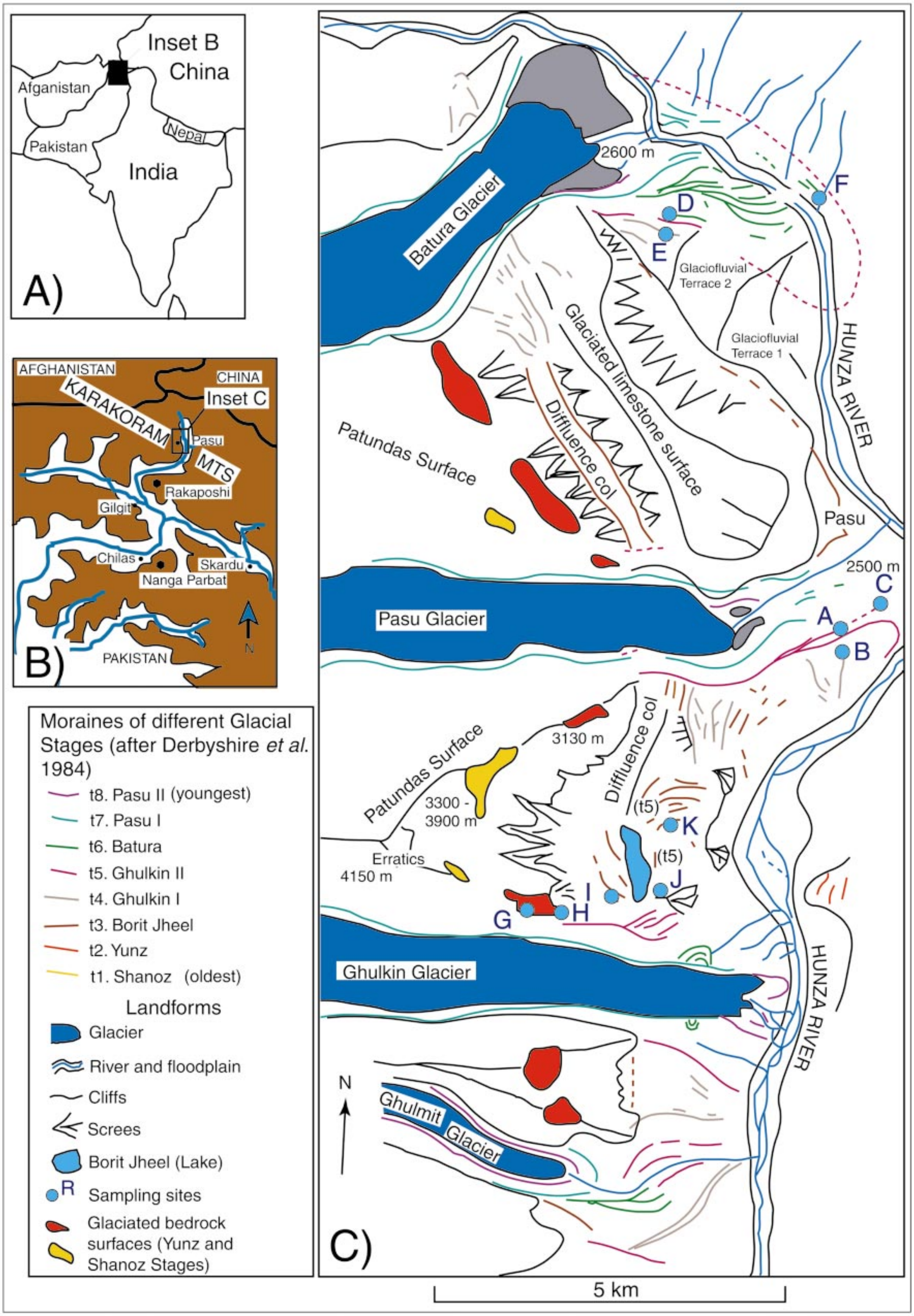
Inset B
China
Afganistan
Nepal
Pakistan
India
A)
AFGHANISTAN
CHINA
KARAKORAM
Inset C
Pasu
MTS
Rakaposhi
Gilgit
Chilas
Skardu
Nanga Parbat
N
PAKISTAN
B)
Moraines of different Glacial Stages (after Derbyshire et al. 1984)
t8. Pasu II (youngest)
t7. Pasu I
t6. Batura
t5. Ghulkin II
t4. Ghulkin I
t3. Borit Jheel
t2. Yunz
t1. Shanoz (oldest)
Landforms
Glacier
River and floodplain
Cliffs
Screes
Borit Jheel (Lake)
R
Sampling sites
Glaciated bedrock surfaces (Yunz and Shanoz Stages)
2600 m
Batura Glacier
D
E
F
Glaciofluvial Terrace 2
Glaciofluvial Terrace 1
Glaciated limestone surface
HUNZA RIVER
Patundas Surface
Diffluence col
Pasu
2500 m
C
A
B
Pasu Glacier
3130 m
Patundas Surface
Diffluence col
3300 - 3900 m
(t5)
K
(t5)
Erratics
4150 m
I
J
G
H
Ghulkin Glacier
HUNZA RIVER
N
Ghulmit Glacier
C)
5 km

Figure 1. (A) and (B) Location of the study area. (C) Simplified geomorphic map of the Batura-Ghulkin area in the Hunza Valley (adapted from Derbyshire et al., 1984). The map shows the locations of the main moraine ridges and glacially eroded surfaces as well as the sampling locations for cosmogenic radionuclide dating.

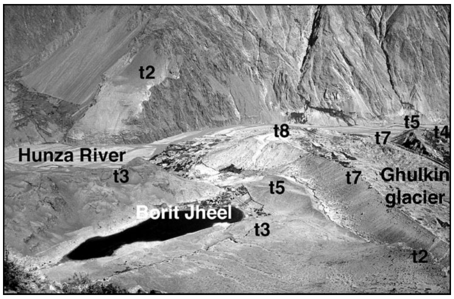

Figure 2. View looking east from an altitude of ~3300 masl on top of a moraine of the Yunz glacial stage, showing the main glacial landforms, the Ghulkin Glacier, and Borit Jheel (lake). Borit Jheel is ~1 km long. The labels t2 to t8 refer to Derbyshire et al.'s (1984) till units (see Table 1).

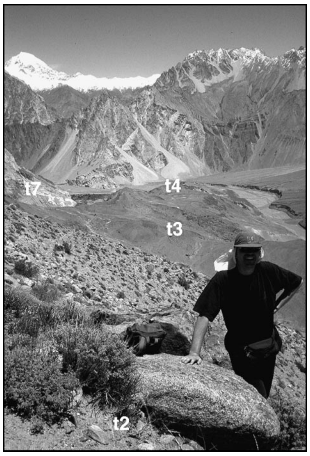

Figure 3. View looking northeast from an altitude of ~3010 masl on top of a moraine of the Yunz glacial stage, showing the diffluence col of the Ghulkin and Pasu glaciers and the main glacial landforms. The boulder in the foreground exemplifies the type of boulders present on the moraines of Yunz age. The labels t2 to t8 refer to Derbyshire et al.'s (1984) till units (see Table 1).

TABLE 1. PREVIOUSLY PROPOSED QUATERNARY GLACIAL STAGES IN THE UPPER HUNZA VALLEY

Till unit	Stage name	Tentative date (yr)*	Description of the glaciations and the main glacial-geologic evidence
t8	Pasu II	Historical (nineteenth and twentieth centuries)	A minor advance of a few hundred meters—sharp-crested, unstable, and sometimes ice-cored moraines with fresh boulders that have no rock varnish
t7	Pasu I	830 ± 80[†] 325 ± 60[†]	A minor advance of ~1 km, restricted to tributary valleys—high, sharp-crested moraines with boulders that have a light yellow surface color
t6	Batura	No dates[§]	A glacial advance of 1–2 km—well-defined moraines with strong varnished and weathered boulders
t5	Ghulkin II	No dates	Minor glacier advance of several kilometers—a multiple series of rounded moraine ridges with deeply weathered boulders having a strong to postmaximal rock varnish, and a weak carbonate development beneath boulders
t4	Ghulkin I	47 000 ± 2 350[#]	Minor valley glaciation, expanding into diffluence cols and into the main Hunza Valley—well-defined moraines with deeply weathered (cavernous) boulders having very strong to postmaximal rock varnish, and incipient calcrete and pendant growth of carbonate
t3	Borit Jheel	65 000 ± 3 300** 50 000 ± 2 500[††]	Main valley glaciations with tributary valley glaciers filling and locally overtopping diffluence cols—highly eroded moraines with deeply weathered boulders having a very strong to postmaximal shiny-black rock varnish, and an extensive underlying calcrete
t2	Yunz	139 000±12 500[§§]	Extensive main valley glaciation—deeply weathered till remnants on benches in the main Hunza Valley at an altitude of ~3900 masl on the upper western slopes of the Pasu-Ghulkin diffluence col
t1	Shanoz	No dates	Extensive broad valley glaciation—deeply weathered erratics on summit surfaces at an altitude of >4150 m asl

Note: This table contains Derbyshire et al.'s (1984) proposed Quaternary glacial stages in the upper Hunza Valley, showing all the dates presented in their work.

*No details of the laboratory procedures used to obtain the dates in China were divulged and so could not be reported in Derbyshire et al. (1984).

[†]Uncalibrated radiocarbon dates on wood from a moraine of the Minapin Glacier, middle Hunza Valley.

[§]Derbyshire et al. (1984) considered this glacial stage to be middle Holocene in age.

[#]Thermoluminescence date on lacustrine silts intercalated with Ghulkin I till of moraines from the Pisan Glacier in the middle Hunza Valley.

**Thermoluminescence date on glaciolacustrine sediments, which were probably deposited during the Borit Jheel Stage, ~1.5 km north of the present snout of the Pasu Glacier.

[††]Thermoluminescence date on glaciotectonized glaciolacustrine sediments within Borit Jheel till ~2.5 km south of the snout of the Batura Glacier.

[§§]Thermoluminescence date on glaciolacustrine silts beneath Borit Jheel till southeast of the Ghulkin I and II Glaciers.

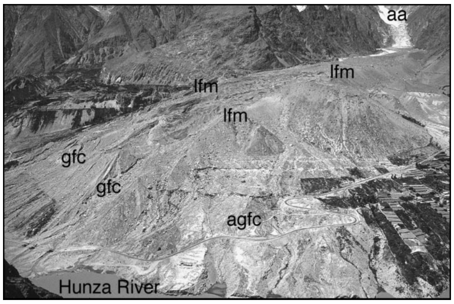

Figure 4. View looking east-southeast across the latero-frontal moraines of the Ghulkin Glacier. The Karakoram Highway runs across the front of this moraine complex. Abbreviations: aa—accumulation area, lfm—crest of the latero-frontal moraine, gfc—active glaciofluvial channel, agfc—abandoned glaciofluvial channel.

has varied by nearly a factor of four, but not in a monotonic fashion. For samples considered in this study, the maximum correction to the exposure age is 12%.

In addition to its intensity, the direction of the dipole field can affect the geomagnetic shielding at a site. Over a sufficiently long time period, the direction of the dipole closely matches that of the geodetic pole. Although there is some uncertainty as to the length of time required for the average of the geomagnetic pole to match that of the axis of rotation, Sternberg (1996) has concluded that the poles are nearly coincident over a period as short as 3000 yr. Because our youngest exposure age is several times longer than this period, we do not consider the effect of apparent polar wander.

We use a SLHL spallogenic-atom production rate of P_n = 5.2 $g^{-1} \cdot yr^{-1}$ for ^{10}Be and P_n = 31.2 $g^{-1} \cdot yr^{-1}$ for ^{26}Al for the exposure-age calculations in this paper. This SLHL produc-

TABLE 2. SAMPLE NUMBERS, LOCATIONS, COSMOGENIC RADIONUCLIDE DATA, AND DATES FOR SAMPLES COLLECTED FROM THE HUNZA VALLEY

Sample number	Latitude ($\pm$0.01°N)	Longitude ($\pm$0.01°E)	Altitude (m)	Shielding factor*	^{10}Be† (10^6 atoms/g)	^{26}Al† (10^6 atoms/g)	Map location	Exposure age(ka)				Glacial stage	Notes**
								^{10}Be†	^{26}Al†	Average§	Geomag corr.#		
KK98-1	36.46	74.90	2550	1	0.423 $\pm$ 0.009	2.69 $\pm$ 0.11	A	13.5 $\pm$ 0.3	14.3 $\pm$ 0.6	13.6 $\pm$ 0.3	13.5 $\pm$ 0.3	Batura (t6)	
KK98-2	36.46	74.90	2550	1	0.295 $\pm$ 0.009	1.58 $\pm$ 0.06	A	9.4 $\pm$ 0.3	8.4 $\pm$ 0.3	9.0 $\pm$ 0.2	9.0 $\pm$ 0.2	Batura (t6)	
KK98-3	36.46	74.90	2550	1	0.471 $\pm$ 0.018	2.41 $\pm$ 0.11	A	15.0 $\pm$ 0.6	12.8 $\pm$ 0.6	13.9 $\pm$ 0.4	13.7 $\pm$ 0.4	Batura (t6)	
KK98-4	36.46	74.90	2550	1	0.333 $\pm$ 0.019	1.60 $\pm$ 0.08	A	10.6 $\pm$ 0.6	8.4 $\pm$ 0.4	9.2 $\pm$ 0.4	9.3 $\pm$ 0.4	Batura (t6)	
KK98-6	36.46	74.90	2640	1	0.829 $\pm$ 0.040	4.77 $\pm$ 0.28	B	25.0 $\pm$ 1.2	24.1 $\pm$ 1.4	24.6 $\pm$ 0.9	23 .2 $\pm$ 0.9	Ghulkin I (t4)	
KK98-7	36.46	74.90	2635	1	0.810 $\pm$ 0.027	4.35 $\pm$ 0.18	B	24.5 $\pm$ 1.2	22.0 $\pm$ 0.9	23.3 $\pm$ 0.6	22.1 $\pm$ 0.6	Ghulkin I (t4)	
KK98-8	36.46	74.90	2640	1	0.915 $\pm$ 0.032	no data	B	27.6 $\pm$ 1.0	no data	27.6 $\pm$ 0.9	25.7 $\pm$ 0.9	Ghulkin I (t4)	
KK98-9	36.46	74.90	2640	1	0.881 $\pm$ 0.034	4.20 $\pm$ 0.19	B	26.6 $\pm$ 1.0	21.1 $\pm$ 0.9	23.6 $\pm$ 0.7	22.4 $\pm$ 0.7	Ghulkin I (t4)	
KK98-10	36.46	74.90	2640	1	0.765 $\pm$ 0.027	4.51 $\pm$ 0.18	B	23.0 $\pm$ 0.8	22.7 $\pm$ 0.9	22.9 $\pm$ 0.6	21.8 $\pm$ 0.6	Ghulkin I (t4)	
KK98-11	36.46	74.90	2540	0.99	0.509 $\pm$ 0.18	2.85 $\pm$ 0.07	C	16.3 $\pm$ 0.6	15.3 $\pm$ 0.4	15.6 $\pm$ 0.3	15.3 $\pm$ 0.3	Ghulkin II (t5)	
KK98-12	36.46	74.90	2540	0.99	0.836 $\pm$ 0.024	4.55 $\pm$ 0.16	C	26.8 $\pm$ 0.8	24.5 $\pm$ 0.8	25.8 $\pm$ 0.6	24.2 $\pm$ 0.5	Ghulkin II (t5)	
KK98-13	36.46	74.90	2540	0.99	0.620 $\pm$ 0.020	3.27 $\pm$ 0.17	C	19.9 $\pm$ 0.6	17.6 $\pm$ 0.9	19.1 $\pm$ 0.5	18.4 $\pm$ 0.5	Ghulkin II (t5)	
KK98-14	36.46	74.90	2540	0.99	0.760 $\pm$ 0.030	4.31 $\pm$ 0.24	C	24.4 $\pm$ 1.0	23.2 $\pm$ 1.3	24.0 $\pm$ 0.8	22.2 $\pm$ 0.7	Ghulkin II (t5)	
KK98-15	36.46	74.90	2550	0.99	0.617 $\pm$ 0.026	3.24 $\pm$ 0.17	C	19.7 $\pm$ 0.8	17.2 $\pm$ 0.9	18.5 $\pm$ 0.6	17.9 $\pm$ 0.6	Ghulkin II (t5)	
KK98-21	36.50	74.87	2660	0.98	0.546 $\pm$ 0.021	2.97 $\pm$ 0.12	D	16.5 $\pm$ 0.6	15.0 $\pm$ 0.6	15.8 $\pm$ 0.5	15.5 $\pm$ 0.4	Ghulkin II (t5)	
KK98-22	36.50	74.87	2670	0.98	0.571 $\pm$ 0.023	2.85 $\pm$ 0.15	D	17.2 $\pm$ 0.7	14.3 $\pm$ 0.7	15.8 $\pm$ 0.5	15.5 $\pm$ 0.5	Ghulkin II (t5)	
KK98-26	36.50	74.87	2740	0.99	0.555 $\pm$ 0.015	3.43 $\pm$ 0.21	E	15.7 $\pm$ 0.4	16.2 $\pm$ 1.0	15.8 $\pm$ 0.4	15.4 $\pm$ 0.4	Ghulkin I (t4)	B**
KK98-34	36.51	74.89	2600	0.99	0.325 $\pm$ 0.011	2.11 $\pm$ 0.11	F	10.0 $\pm$ 0.3	10.9 $\pm$ 0.5	10.0 $\pm$ 0.3	10.3 $\pm$ 0.3	Batura (t6)	
KK98-34	36.51	74.89	2610	0.99	0.373 $\pm$ 0.014	1.91 $\pm$ 0.10	F	11.4 $\pm$ 0.4	9.7 $\pm$ 0.5	10.8 $\pm$ 0.3	10.8 $\pm$ 0.3	Batura (t6)	E
KK98-35	36.51	74.89	2595	0.99	0.369 $\pm$ 0.014	1.86 $\pm$ 0.11	F	11.4 $\pm$ 0.4	9.6 $\pm$ 0.6	10.7 $\pm$ 0.3	10.7 $\pm$ 0.3	Batura (t6)	
KK98-42	36.43	74.84	3310	0.99	1.91 $\pm$ 0.08	10.6 $\pm$ 0.4	G	38.7 $\pm$ 1.6	36.0 $\pm$ 1.3	37.0 $\pm$ 1.0	32.8 $\pm$ 0.9	Yunz (t2)	C
KK98-43	36.43	74.84	3310	0.99	1.41 $\pm$ 0.05	7.34 $\pm$ 0.31	G	28.4 $\pm$ 1.0	24.8 $\pm$ 1.0	26.7 $\pm$ 0.7	25.0 $\pm$ 0.7	Yunz (t2)	C
KK98-44	36.43	74.84	3250	0.99	1.22 $\pm$ 0.03	6.70 $\pm$ 0.19	H	25.5 $\pm$ 0.5	23.5 $\pm$ 0.7	24.7 $\pm$ 0.4	23.2 $\pm$ 0.4	Yunz (t2)	C
KK98-45	36.43	74.84	3250	0.99	2.11 $\pm$ 0.04	12.0 $\pm$ 0.3	H	44.2 $\pm$ 0.9	42.3 $\pm$ 1.2	43.5 $\pm$ 0.7	38.4 $\pm$ 0.6	Yunz (t2)	C
KK98-46	36.43	74.84	3250	0.99	1.62 $\pm$ 0.04	9.05 $\pm$ 0.44	H	33.8 $\pm$ 0.9	31.8 $\pm$ 1.5	33.4 $\pm$ 0.8	30.4 $\pm$ 0.7	Yunz (t2)	C
KK98-47	36.43	74.84	3180	0.99	2.38 $\pm$ 0.06	12.3 $\pm$ 0.5	I	52.1 $\pm$ 1.3	45.2 $\pm$ 1.9	50.0 $\pm$ 1.1	43.2 $\pm$ 0.9	Borit Jheel (t3)	D
KK98-50	36.43	74.84	3180	0.98	2.85 $\pm$ 0.07	15.7 $\pm$ 0.7	I	63.8 $\pm$ 1.6	60.0 $\pm$ 2.5	62.6 $\pm$ 1.3	54.7 $\pm$ 1.2	Borit Jheel (t3)	
KK98-55	36.44	74.87	2760	1	2.00 $\pm$ 0.06	10.5 $\pm$ 0.8	J	56.3 $\pm$ 1.8	49.8 $\pm$ 3.8	55.1 $\pm$ 1.6	47.9 $\pm$ 1.4	Borit Jheel (t3)	F
KK98-56	36.44	74.87	2720	1	1.92 $\pm$ 0.04	11.6 $\pm$ 0.3	J	55.5 $\pm$ 1.1	56.6 $\pm$ 1.6	55.8 $\pm$ 0.9	48.5 $\pm$ 0.8	Borit Jheel (t3)	F
KK98-57	36.44	74.87	2760	1	1.97 $\pm$ 0.03	10.3 $\pm$ 1.7	J	55.5 $\pm$ 1.0	49.1 $\pm$ 8.1	55.4 $\pm$ 1.0	48.1 $\pm$ 0.8	Borit Jheel (t3)	F
KK98-64	36.43	74.86	2660	0.99	0.997 $\pm$ 0.025	5.47 $\pm$ 0.35	K	29.7 $\pm$ 0.7	27.3 $\pm$ 1.8	29.4 $\pm$ 0.7	27.1 $\pm$ 0.6	Borit Jheel (t3)	B
KK98-65	36.43	74.87	2680	0.99	1.36 $\pm$ 0.03	7.97 $\pm$ 0.28	K	40.0 $\pm$ 0.8	39.6 $\pm$ 1.4	39.9 $\pm$ 0.7	35.8 $\pm$ 0.6	Borit Jheel (t3)	B

Note: See Figure 1 for the sample locations.

*The topographic shielding factor was determined by using the methods of Nishiizumi et al. (1989).

†Uncertainty includes only uncertainty in AMS measurement.

§Weighted average of ^{10}Be and ^{26}Al age. The uncertainty is the larger of the propagated uncertainty and the standard deviation of the two ages.

#Corrected for time-varying geomagnetic field as described in text. The uncertainty is carried over from that in the average exposure age. No additional uncertainty was assigned arising from correction for geomagnetic-field change.

**B—deeply weathered and exfoliated boulder; C—deeply weathered and unstable boulder; D—dip correction made for a tilted boulder surface by using the methods of Nishiizumi et al. (1989); E—repeat sample; F—sample from a striated bedrock surface.

tion rate for ^{10}Be is the 13 000 yr rescaled measurement from glacial surfaces in the Sierra Nevada (Nishiizumi et al., 1989). This result is very similar to that determined on the 9800 yr Köfels landslide (Kubik et al., 1998). When corrected for time variation in the geomagnetic field for >13 000 yr, as just described, the P_n value for ^{10}Be increases to 5.4 $g^{-1} \cdot yr^{-1}$. The SLHL P_n for ^{26}Al is calculated as the product of the SLHL P_n for ^{10}Be and the spallogenic-production-rate ratio of ^{26}Al/^{10}Be, which we take to be 6.03 $\pm$ 0.31 from data reported in the Sierra Nevada calibration study. To rescale the Sierra Nevada production rates, we used ^{10}Be concentrations reported by Nishiizumi et al. (1989), revised glacial-retreat ages reported by Clark et al. (1995), the star production rates from Table 2 in Lal (1991), and, as suggested by Nishiizumi et al. (1996), the geographic latitude of the calibration samples. The Sierra Nevada production rate was rescaled from the measured altitudes and latitudes as previously discussed, under the assumption that at sea level, muon reactions contribute only ~3% to ^{10}Be and ^{26}Al production in quartz. There are, to our knowledge, only two other published estimates of ^{10}Be production rates: (1) from the Laurentide ice retreat in New Jersey (Clark et al., 1995) and (2) from glacial retreat in Scotland (Stone et al., 1998a). Both of these estimates yield SLHL production rates somewhat lower than the two high-altitude results. Because the Hunza samples more closely match the altitude and latitude of the Sierra Nevada site, we have chosen to use production rates calculated from measurements at this site to calculate the exposure ages of our samples.

RESULTS

The ^{10}Be and ^{26}Al concentrations we measured (Table 2) allow us to calculate model exposure ages that specify the late glacial chronology of the Hunza region. In most instances, both ^{10}Be and ^{26}Al were measured. For each sample, the dates obtained by using the different cosmogenic radionuclides are consistent; however, the ^{26}Al ages are systematically slightly younger for reasons that are unexplained. We tend to be more confident of the ^{10}Be ages than of the ^{26}Al ages because the former rely on a single measurement, ^{10}Be/Be, whereas the latter requires two measurements, ^{26}Al/Al and Al concentration. However, lacking conclusive grounds to prefer one over the other, we have chosen to use the mean of the ^{26}Al and ^{10}Be ages when presenting age ranges for each glacial stage. These ages are calculated under the assumption of a zero erosion rate. Ages are calculated both without and with correction for geomagnetic-field variation over time. The effect of the time-varying geomagnetic field only becomes significant for samples of Borit Jheel age. We have not endeavored to calculate the uncertainty of this correction and have simply propagated the uncertainty from the uncorrected age. In the following discussion, we rely on the corrected ages because we consider these to be the best estimates of the exposure ages of the samples.

Erosion rates have not been measured at our site. Small et al. (1997), however, determined a maximum mean erosion rate for alpine bedrock summit surfaces in four U.S. mountain ranges of 7.6 ± 3.9 m·m.y.$^{-1}$ and argued that summit-surface erosion rates in other environments, except extremely arid regions, are of this magnitude. The Karakoram Mountains are more arid than the study areas in the western United States. In addition, for dating the Hunza moraines, we selected large boulders that stand above the general topography. This choice suggests that these boulders are likely to have low erosion rates. Both of these factors make it likely that rates of erosion of the Hunza Valley moraine boulders are <7.6 m·m.y.$^{-1}$. For erosion rates of 1–5 m·m.y.$^{-1}$, an age of 10 ka calculated assuming zero erosion would underestimate the true age by 1%–4%; an age of 20 ka, by 2%–9%; and an age of 40 ka, by 4%–20%. The existence of glacial striations on bedrock exposed at Borit Jheel (samples KK98–55, KK98–56, and KK98–57) and the general agreement (~12%) in the ages of these bedrock samples and two associated boulders (KK98–47 and KK98–50) further supports the conclusion that erosion has been in the 1–5 m·m.y.$^{-1}$ range.

Episodic mass wasting caused by frost action or fire spalling should be stochastic, affecting each boulder differently. The concordance in age between individual boulders from the same moraine indicates that such events are scarce. The calculated exposure ages are plotted in Figure 5A according to their location and relative age.

The cosmogenic radionuclide dates define the timing of four glacial stages and, because of the uncertain effects of erosion, minimum ages for the oldest glacial stage. The ages for each glacial stage are summarized in the following sections. These ages have been corrected for the effect of the varying geomagnetic field as previously discussed.

Batura Glacial Stage

Six boulders were dated from moraines belonging to the Batura glacial stage. These are located at map positions A and F (Fig. 1). Ages of five of the boulders cluster between 9.0 and 10.8 ka. Effects of erosion are negligible over this time span. Two boulders (KK98–1 and KK98–3) have greater ages, both ca. 13 ka. It is likely that these boulders were incorporated from an older Ghulkin II age moraine that has a similar age. This conjecture is possible because progressively younger advances produce moraines inset within older moraines and the younger moraines could possibly incorporate older moraine boulders. The Batura glacial stage represents an early Holocene advance.

Ghulkin II Glacial Stage

Seven Ghulkin II Stage boulders were dated. These are located on the map at positions C and D (Fig. 1). The exposure ages range between 15.3 and 18.4 ka. Two boulders (KK98–12 and KK98–14) have outlier ages at ca. 24–22 ka. Like the aforementioned Batura outliers, these two boulders have ages consistent with having been derived from an older moraine, in this case from a Ghulkin I moraine. The Ghulkin II glacial stage predates the Late Glacial interstadial (Bølling-Ållerød).

Ghulkin I Glacial Stage

Six boulders from moraines belonging to the Ghulkin I glacial stage were dated. These are located at map positions B and E (Fig. 1). The ages range between 21.8 and 25.7 ka, a tight clustering, with an outlier at location E having an age of 15.4 ka. This glaciation broadly correlates with the global Last Glacial Maximum in marine oxygen isotope stage 2 (MIS 2). Likely erosion effects, up to ~10%, do not affect this conclusion. Our cosmogenic radionuclide ages for the Ghulkin I glacial stage disagree with Derbyshire et al.'s (1984) TL date of 47 ± 2.35 ka. The disagreement in ages may indicate that the sediment that was TL dated was partly bleached. Such an effect would give an age much older than the true age of deposition. Partial bleaching is quite common in high-energy mountain environments where sediments are carried in turbid streams and are deposited rapidly (cf. Richards, 2000).

Borit Jheel Glacial Stage

The ages for the four boulders and three bedrock surfaces of Borit Jheel glacial age range between 43.2 and 54.7 ka. These are located at map positions I, J, and K. The bedrock samples retained glacial striae and therefore have been subject to minimal erosion. These results suggest that the Borit Jheel glacial stage occurred at ca. 48 ka or somewhat earlier. These cosmogenic radionuclide ages are in broad agreement with the TL dates of 65 ± 3.3 ka and 50 ± 2.5 ka (Derbyshire et al., 1984). There are two anomalies (KK98–64 and KK98–65) with ages of ca. 27 ka and ca. 35 ka. The young ages on these boulders may be the result of deep weathering and exfoliation. The Borit Jheel glacial stage represents a glacial advance that occurred during MIS 3.

Yunz Glacial Stage

All the exposure ages for the five boulders associated with the Yunz glacial event have younger apparent exposure ages than boulders from the Borit Jheel glacial stage. These young ages are inconsistent with morphostratigraphic field relationships. The boulders associated with the Yunz glacial advance may have spalled or toppled during their long exposure, thereby exposing new surfaces to cosmic rays. The spalling or toppling of boulders is likely to become more important with age as the landscape denudes. The Yunz glacial stage, exposure ages notwithstanding, was probably an extensive glacial event (Derbyshire et al., 1984) that occurred during the early part of the last glacial cycle or during a previous glacial cycle.

DISCUSSION

The glacial-geologic record in the upper Hunza Valley provides evidence of at least six glacial advances since ca. 60 ka. The age of four of these glacial advances has been defined by cosmogenic radionuclide exposure-age dating (Fig. 5A). Derbyshire et al. (1984) showed, on the basis of radiocarbon dating, that the two youngest glacial advances (Pasu I and Pasu II glacial stages) occurred during the past few hundred years. The young ages for the oldest glacial stage that we attempted to date, the Yunz glacial stage, showed that in this region, moraine and boulder erosion on deposits that are older than the Borit Jheel glacial stage (>60 ka) make it difficult to find pristine boulders for cosmogenic radionuclide dating.

It is difficult to correlate the Hunza glacial successions with specific dated climatic events. On a global scale, there are the well-documented warming and cooling cycles responsible for changes in the oxygen isotope records in marine sediments and polar ice cores (Bond et al., 1993). Global warming intensifies the southwest Asian monsoon, leading to an increase and a farther-north penetration of monsoon-derived moisture (Sirocko et al., 1991). Benn and Owen (1998) speculated that glaciation in the northwest Himalaya and Trans-Himalaya is especially sensitive to northward penetration of monsoon-derived moisture. However, during times of increased moisture, temperatures are also generally higher. In addition to these changes in the monsoon, there are cooling events associated

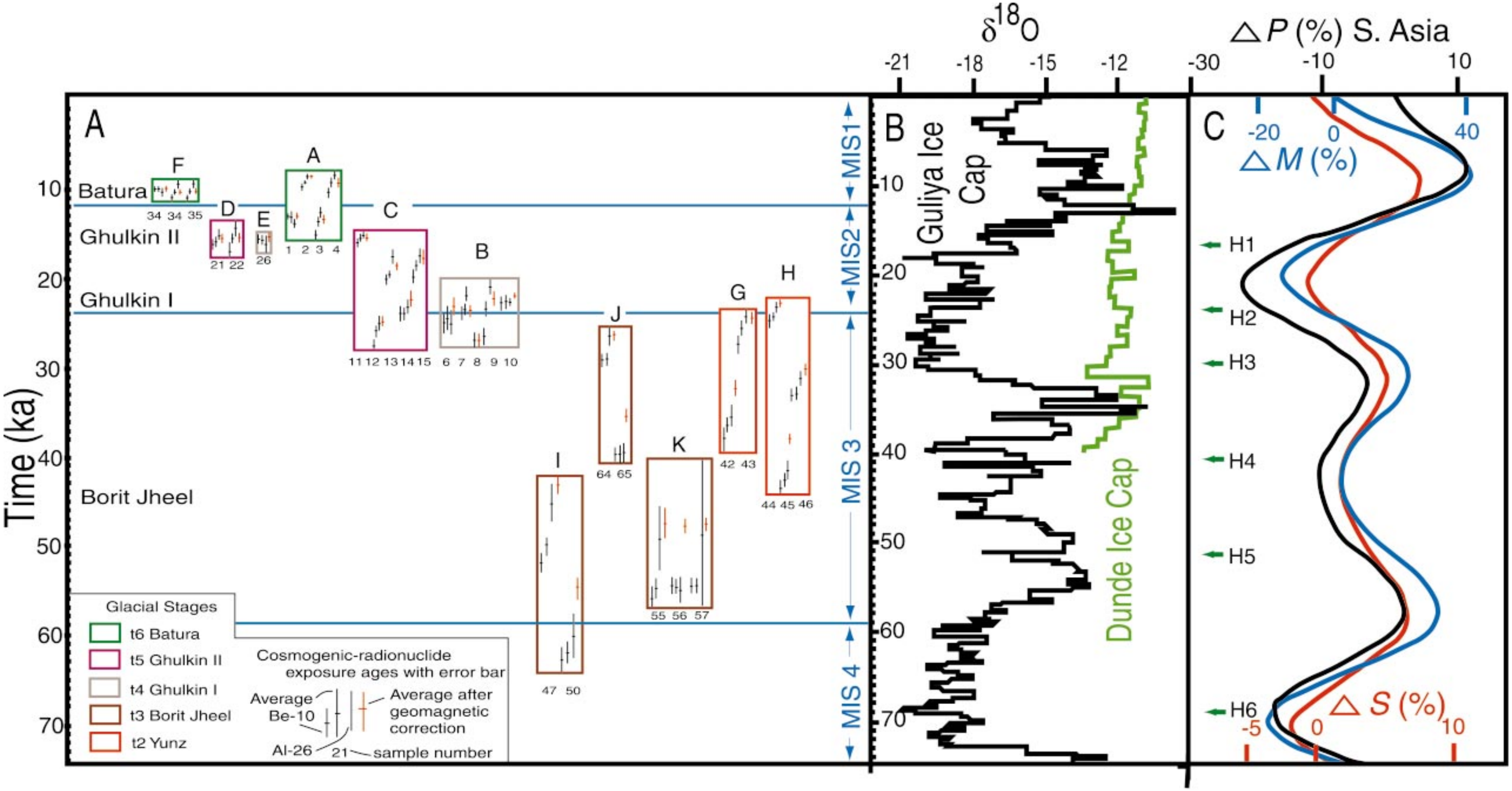

Figure 5. (A) Cosmogenic radionuclide ages for moraines in the Hunza Valley. (B) δ18O data from cores of the Dunde ice cap and the Guliya ice cap in Tibet (Thompson et al., 1989, 1997). (C) Simulated monsoon pressure index (Δ*M* percentage, solid blue line) for the Indian Ocean and simulated changes in precipitation (Δ*P* percentage, black line) in southern Asia (Prell and Kutzbach, 1987), and variations in Northern Hemisphere solar radiation (Δ*S* percentage, dashed blue line; Prell and Kutzbach, 1987). H1, H2, H3, H4, and H5 show the timing of Heinrich events during the past 70 ka (Bond et al., 1992). The cosmogenic radionuclide ages are plotted along the *x*-axis according to their geographical locations (A to K) and their relative ages (see Fig. 1 and Table 2 for the exact locations). Locations A to C, D to F, and G to K are associated with the Pasu, Batura, Ghulkin Glaciers, respectively. Each colored box encloses samples from the same moraine. The blue horizontal lines represent the boundaries of the marine oxygen isotope stages (MISs), and are taken from Martinson et al. (1987) and Shackleton et al. (1990).

with increased ice rafting in the North Atlantic, the Heinrich events. By using cosmogenic radionuclide ^{36}Cl dating, Phillips et al. (1996) showed that multiple glacial advances in the Sierra Nevada were approximately coincident with Heinrich events 5, 3, 2, and 1 and that glaciations in this region may be temporally related to climatic cycles in the North Atlantic. Our data suggest that in the Karakoram, both monsoon and North Atlantic climate serve to influence the extent of glaciation.

Glacial advance in the Karakoram results from changes in temperature and precipitation. Both of those in turn are controlled by variations in the southwest Asia summer monsoon. The Ghulkin I and Ghulkin II glacial stages occurred during periods of decreased precipitation associated with one weakening of the southwest Asia monsoon (Fig. 5). The Ghulkin I and Ghulkin II advances might, likewise, correlate with Heinrich events 2 and 1, respectively. If this is the case, it is likely that these advances are associated with a Northern Hemisphere cooling. The Ghulkin advances are relatively restricted in extent (Fig. 6), suggesting that temperatures were probably low enough to allow glaciers to advance into the Hunza Valley and spill over into diffluence cols (Fig. 6) even though precipitation was reduced. Evidently, precipitation supply was insufficient to permit the glaciers to descend far into the main valley.

The Borit Jheel glacial stage, on the other hand, occurred during MIS 3 when the southwest Asia summer monsoon was strengthened relative to its earlier and later intensity in MIS 2 or MIS 4 (Prell and Kutzbach, 1987) (Fig. 5). We expect that during such periods of increased intensity, the southwest Asian summer monsoon penetrates farther into the Karakoram Mountains and causes an increase in summer snowfall at high altitudes. The resultant positive mass balances in the glaciers of the Greater Himalaya and Karakoram Mountains can cause the glaciers to advance, as long as temperatures are not so high that meltwater runoff predominates. In fact, examination of Figure 5 shows that the large Borit Jheel advance occurred during a slight weakening in the strong MIS 3 monsoon (ca. 50–40 ka). Evidently, conditions for glaciation were optimal not at the peak of the monsoon, but rather during a period of relative monsoonal weakening. The combination of somewhat cooler temperatures with increased precipitation rates allowed the Hunza glaciers to advance well into the main valley during Borit Jheel time. Thompson et al. (1997) provided additional evidence for an interstadial during MIS 3 from an ice-core record from the Guliya ice cap in western Tibet. The Borit Jheel glacial advance supports Benn and Owen's (1998) hypothesis that the local Last Glacial Maximum in many parts of the Himalaya may have occurred early in the last glacial cycle and that this glacial maximum in the region was asynchronous with oscillations in the Northern Hemisphere ice sheets and oceans.

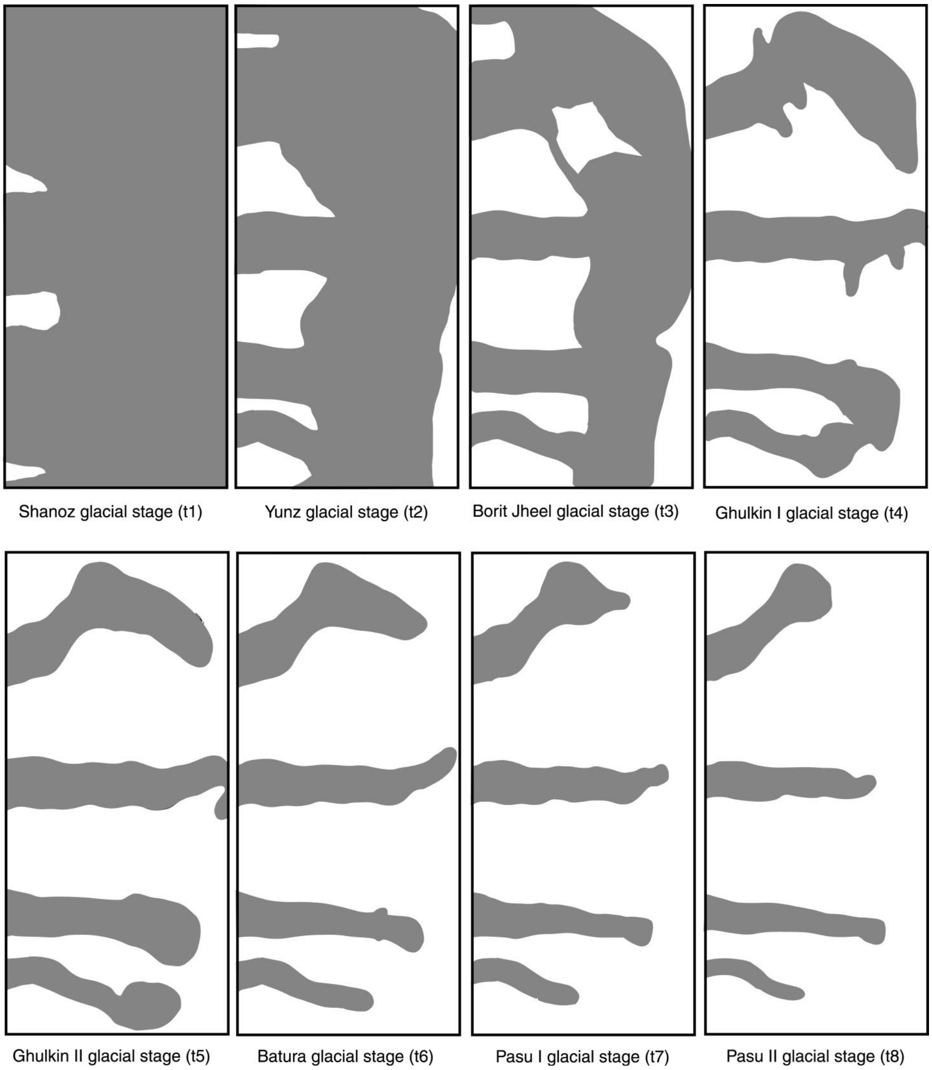

Figure 6. The extent of glaciation in the Batura-Ghulkin area of the upper Hunza Valley in each of Derbyshire et al.'s (1984) glacial stages. The reconstructions are based on our modified version of Derbyshire et al.'s (1984) geomorphic map; the area covered is the same as that shown in Figure 1C.

The Batura glacial stage represents a minor glacial advance in the early Holocene (10.8–9.0 ka). This advance was probably associated with increased precipitation in a strengthened southwest Asian summer monsoon during the early Holocene insolation maximum. Lacustrine sediments and shorelines in western Tibet testify to warmer and wetter conditions than at present during the early Holocene–middle Holocene (Gasse et al., 1991). Phillips et al. (2000) showed that glaciers were advancing in the Nanga Parbat region during the early Holocene–middle Holocene (ca. 9.0–5.5 ka), and they attributed the glacial advances to a strengthened southwest Asian summer monsoon.

Although uncertainties in the surface-exposure ages preclude definitive conclusions, the data suggest a correlation between glacial advances in the Karakoram Mountains and Heinrich events in the North Atlantic. The Borit Jheel, Ghulkin I, and Ghulkin II advances correlate well with Heinrich events 5–4, 2, and 1. There is no glacial advance associated with Heinrich event 3, which occurred near a peak in the MIS 3 monsoon in-

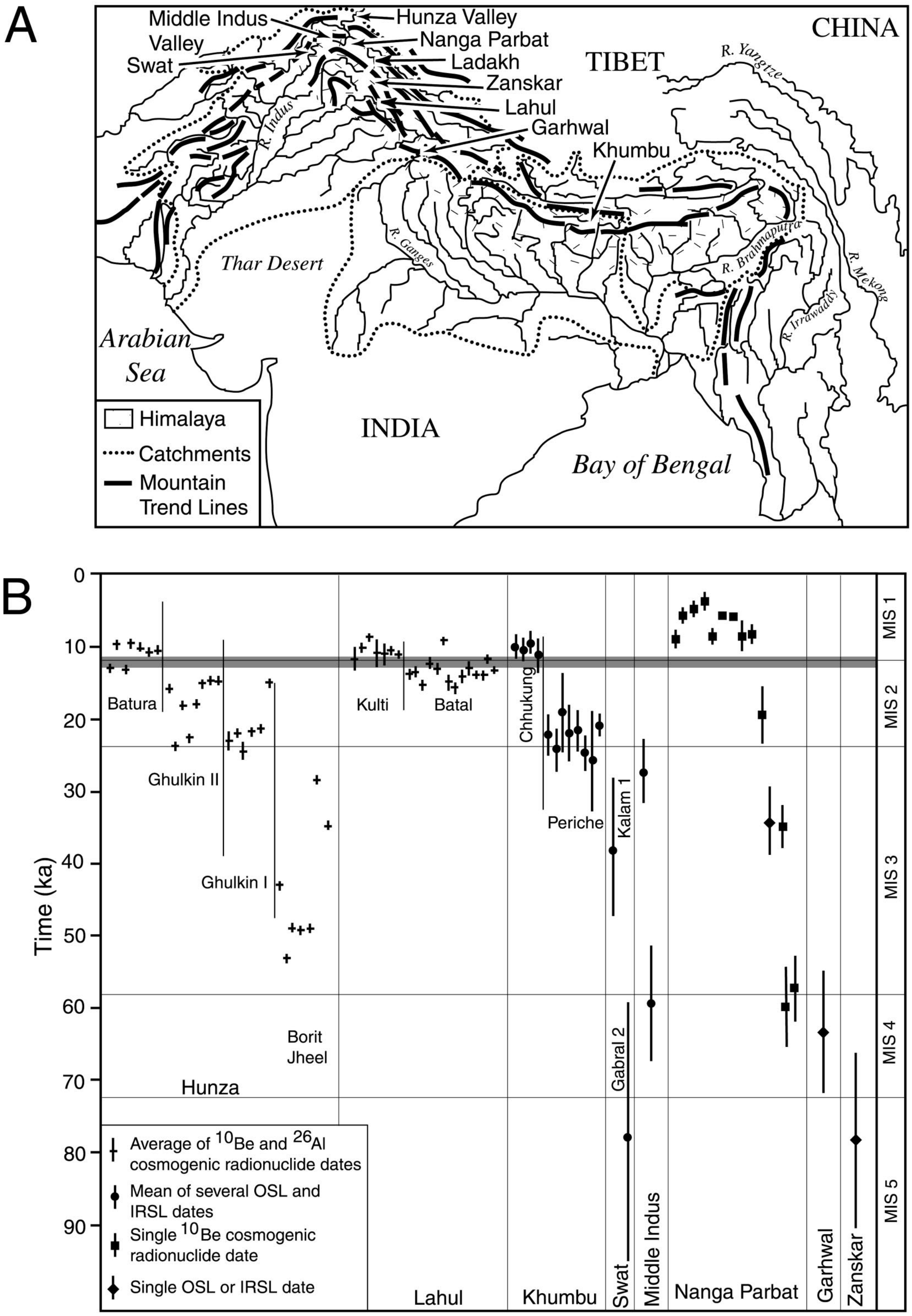

Figure 7. Cosmogenic radionuclide and OSL (optically stimulated luminescence: green light and/or blue light) and IRSL (infrared stimulated luminescence) dates for glacial chronologies throughout the Himalaya. These include all the published dates that are considered reliable, that is, those for which full methodological and analytical descriptions have been provided. (A) The locations of each study region. (B) Comparison of dates. Different glacial stages are illustrated within each region. The data have been compiled from Owen et al. (2001), Richards et al. (2000, 2001), Sharma and Owen (1996), Phillips et al. (2000), and Taylor and Mitchell (2000). Note that only two dates are presented for the Garhwal Himalaya; although Sharma and Owen (1996) published five dates, only two of their dates really defined the timing of glaciations in this region. The horizontal gray bar illustrates the duration of the Younger Dryas Stade. The boundaries of the marine oxygen isotope stages (MISs) are taken from Martinson et al. (1987) and Shackleton et al. (1990).

tensity. If there is a correlation with Heinrich events, it appears that the associated cooling was not sufficient to overcome the warming associated with this maximum in the monsoon.

Comparison of the Hunza Valley glacial chronology with that of other regions throughout the Himalaya shows that, for most regions, the local Last Glacial Maximum occurred early in the last glacial cycle (Fig. 7). In the Swat Himalaya and the Zanskar Valley, the local Last Glacial Maximum occurred during MIS 5a (Richards et al., 2000; Taylor and Mitchell, 2000), whereas in Nanga Parbat and the Middle Indus Valley, the local maximum probably occurred during MIS 3 (Richards et al., 2000; Phillips et al., 2000; Taylor and Mitchell, 2000). The ice-core record from the Guliya ice cap supports the view that interstadial conditions existed in western Tibet during MISs 5c, 5a, and 3 (Thompson et al., 1997). The Last Glacial Maximum in the Garhwal Himalaya has been assigned to MIS 4, although the large error bars associated with the OSL (optically stimulated luminescence) date suggest that it could have occurred during MIS 3 (Sharma and Owen, 1996). Extensive early glaciations have also been recognized in the Khumbu Himal and Lahul Himalaya, but these have not been defined by numerical dating (Richards et al., 2001; Owen et al., 2001).

The glacial chronologies in Khumbu Himal, Nanga Parbat, and the Garhwal and Swat Himalaya compare well with the Hunza data showing that the maximum extent of glaciation in the Hunza Valley occurred during the earlier part of the last glacial cycle. It is conceivable that the Yunz glacial stage is coincident with MISs 5a or 5c. During these times the monsoon would have been strengthened and would have increased snowfall at high altitudes, and yet it would have been cold enough to cause a positive mass balance in the glacial systems, allowing glaciers to advance. Alternatively, the Yunz glacial stage may have occurred during an earlier glacial cycle.

The Ghulkin I glacial stage, contemporaneous with the global Last Glacial Maximum, compares well with the Periche glacial stage in the Khumbu Himal (Richards et al., 2001). Furthermore, by using OSL dating, Richards et al. (2000) showed that glaciers had advanced into the Indus Valley during MIS 2. However, Phillips et al. (2000) argued that the lack of cosmogenic radionuclide ages from the Nanga Parbat massif in MIS 2 provides evidence that Nanga Parbat was too arid to support expanded ice during this period of low monsoon intensity. Our cosmogenic radionuclide dates in the Hunza Valley suggest a limited advance during MIS 2 (Fig. 6). These data are consistent with the conclusions of Richards et al. (2000) and are by no means inconsistent with the data of Phillips et al. (2000).

There is no glaciation equivalent to the Ghulkin II glacial stage in any other part of the Himalaya. In contrast, the Batal glacial stage in the Lahul Himalaya (Owen et al., 2001) occurred during the late glacial interstadial (Bølling/Ållerød), not prior to the late glacial interstadial as in the case of the Ghulkin II glacial stage. However, the early Holocene glacial advance recognized in the Hunza Valley (Batura glacial stage) is broadly synchronous with advances in the Lahul Himalaya (Kulti glacial stage), the Khumbu Himal (Chhukung glacial stage), and Nanga Parbat region (Owen et al., 2001; Richards et al., 2000; Phillips et al., 2000). These data, when taken together, show that glaciations across the Himalaya appear to be broadly synchronous.

CONCLUSIONS

Cosmogenic radionuclide ^{10}Be and ^{26}Al date glacial landforms back to ca. 60 ka in the Karakoram Mountains. The oldest glacial stages—the Shanoz and Yunz glacial stages—are older than 60 ka and may have occurred during the early part of the last or penultimate glacial cycles. Cosmogenic radionuclide dates on the Borit Jheel, Ghulkin I, Ghulkin II, and Batura glacial stages date these glacial advances to ca. 54.7–43.2 ka, ca. 25.7–21.8 ka, ca. 18.4–15.3 ka, and ca. 10.8–9.0 ka, respectively. The two youngest glacial advances, the Pasu I and II glacial stages, occurred during the past few hundred years (Derbyshire et al., 1984).

Glaciation in the Hunza Valley became progressively less extensive throughout the last glacial cycle. The local Last Glacial Maximum occurred early in the last glacial cycle, but it is not possible to resolve whether this event was during the Borit Jheel, Yunz, or Shanoz glacial stages because the latter two glacial stages have not been adequately dated.

Uncertainties in cosmogenic radionuclide production rates and in the exposure history of exposed rock surfaces make it impossible at this time to describe unambiguously the climate mechanisms that control the pattern of glaciations in this region. However, our data set suggests that late Quaternary glacial advances in the Karakoram Mountains did not occur at the peak of southwest Asian monsoon intensity. In addition, there is a suggestion that the North Atlantic cooling associated with Heinrich events was coincident with glacial advances in the Karakoram Mountains. Further refinement of the chronology will be necessary to test this suggestion. In addition, our numerical dates provide a geochronological framework that may be used when examining late Quaternary glacial chronologies from other areas of the Karakoram and adjacent mountains.

ACKNOWLEDGMENTS

We acknowledge support from the Institute of Geophysics and Planetary Physics (IGPP) at the Lawrence Livermore National Laboratory, operating under the auspices of U.S. Department of Energy contract EN6–7405, and the University Collaborative Research Program of IGPP for funding this research. We thank Edward Derbyshire, Paul Bierman, Fred Phillips, and an anonymous reviewer for their constructive and positive comments on our paper.

REFERENCES CITED

Andrews, J.T., 1975, Glacial systems: North Scituate, Massachusetts, Duxbury, 191 p.

Batura Glacier Investigation Group, 1979, The Batura glacier in the Karakoram Mountains: Scientia Sinica, v. 22, p. 281–293.

Benn, D.I., and Owen, L.A., 1998, The role of the Indian summer monsoon and the mid-latitude westerlies in Himalayan glaciation: Review and speculative discussion: London, Journal of the Geological Society, v. 155, p. 353–363.

Bond, G., Heinrich, H., Broecker, W., Labeyrie, L., McManus, J., Andrews, J., Huon, S., Jantschik, R., Clasen, S., Simet, C., Tedesco, K., Klas, M., Bonani, G., and Ivy, S., 1992, Evidence for massive discharges of icebergs into the North Atlantic during the last glacial period: Nature, v. 360, p. 245–249.

Bond, G., Broecker, W., Labeyrie, L., McManus, J., Jouzel, J., and Bonani, G., 1993, Correlations between climate records from North Atlantic sediments and Greenland ice: Nature, v. 365, p. 143–147.

Bradley, R.S., 1999, Paleoclimatology: Boston, Massachusetts, Harcourt Academic Press, 513 p.

Brown, E.T., Brook, E.J., Raisbeck, G.M., Yiou, F., and Kurz, M.D., 1992, Effective attenuation of cosmic rays producing ^{10}Be and ^{26}Al in quartz: Implications for exposure dating: Geophysical Research Letters, v. 19, p. 369–372.

Clark, D.H., Bierman, P.R., and Larsen, P., 1995, Improving in situ cosmogenic chronometers: Quaternary Research, v. 44, p. 367–377.

Collins, D.N., 1998, Suspended sediment flux in meltwaters draining from the Batura glacier as an indicator of the rate of glacial erosion in the Karakoram Mountains: Quaternary Proceedings, v. 6, p. 1–10.

Davis, J.C., Proctor, I.D., Southon, J.R., Caffee, M.W., Heikkinen, D.W., Roberts, M.L., Turteltaub, K.W., Nelson, D.E., Loyd, D.H., and Vogel, J.S., 1990, LLNL/UC AMS facility and research program: Nuclear Instruments and Methods in Physics Research, v. B52, p. 269–272.

Derbyshire, E., and Owen, L.A., 1997, Quaternary glacial history of the Karakoram Mountains and northwest Himalayas: A review: Quaternary International, v. 38/39, p. 85–102.

Derbyshire, E., Li Jijun, Perrott, F.A., Xu Shuying, and Waters, R.S., 1984, Quaternary glacial history of the Hunza Valley, Karakoram Mountains, Pakistan, *in* Miller, K., ed., International Karakoram Project: Cambridge, UK, Cambridge University Press, p. 456–495.

Dunai, T.J., 2000, Scaling factors for production rates of in situ produced cosmogenic nuclides: A critical reevaluation: Earth and Planetary Science Letters, v. 176, p. 157–169.

Gasse, F., Arnold, M., Fontes, J.C., Fort, M., Gibert, E., Huc, A., Li, B., Li, Y., Liu, Q., Melieres, F., Van Campo, E., Wang, F., and Zhang, Q., 1991, A 13,000-year climate record from western Tibet: Nature, v. 353, p. 742–745.

Gosse, J.C., Evenson, E.B., Klein, J., Lawn, B., and Middleton, R., 1995a, Precise cosmogenic ^{10}Be measurements in western North America: Support for a global younger Dryas cooling event: Geology, v. 23, p. 877–880.

Gosse, J.C., Klein, J., Evenson, E.B., Lawn, B., and Middleton, R., 1995b, Beryllium-10 dating of the duration and retreat of the Last Pinedale glacial sequence: Science, v. 268, p. 1329–1333.

Goudie, A.S., Brunsden, D., Collins, D.N., Derbyshire, E., Ferguson, R.I., Hashnet, Z., Jones, D.K.C., Perrott, F.A., Said, M., Waters, R.S., and Whalley, W.B., 1984, The geomorphology of the Hunza Valley, Karakoram Mountains, Pakistan, *in* Miller, K., ed., International Karakoram Project: Cambridge, UK, Cambridge University Press, p. 411–455.

Granger, D.E., and Smith, A.L., 2000, Dating buried sediments using radioactive decay and muogenic production of ^{10}Be and ^{26}Al: Nuclear Instruments and Methods, B, v. 172, p. 822–826.

Granger, D.E., Riebe, C.S., Kirchner, J.W., Finkel, R.C., 2001, Modulation of erosion on steep granite slopes by boulder armoring, as revealed by cosmogenic ^{26}Al and ^{10}Be: Earth and Planetary Science Letters, v. 186, p. 269–281.

Guyodo, Y., and Valet, J.-P., 1996, Relative variation in geomagnetic intensity from sedimentary records: The past 200,000 years: Earth and Planetary Science Letters, v. 176, p. 23–36.

Heisinger, B.P., 1998, Myonen-induzierte Produktion von Radionukliden [Ph.D. thesis]: Munich, Germany, Technische Universität München, 153 p.

Heisinger, B., and Nolte, E., 2000, Cosmogenic in situ production of radionuclides: Exposure ages and erosion rates: Nuclear Instruments and Methods in Physics Research, B, v. 172, p. 790–795.

Hewitt, K., 1988, Catastrophic landslide deposits in the Karakoram Himalaya: Science, v. 242, p. 64–77.

Kohl, C.P., and Nishiizumi, K., 1992, Chemical isolation of quartz for measurement of in situ–produced cosmogenic nuclides: Geochimica et Cosmochimica Acta, v. 56, p. 3583–3587.

Kubik, P.W., Ivy-Ochs, S., Masarik, J., Frank, M., and Schlüchter, C., 1998, ^{10}Be and ^{26}Al production rates deduced from an instantaneous event within the dendro-calibration curve, the landslide of Köfels, Ötz Valley, Austria: Earth and Planetary Science Letters, v. 161, p. 231–241.

Lal, D., 1991, Cosmic ray labeling of erosion surfaces: In situ nuclide production rates and erosion models: Earth and Planetary Science Letters, v. 104, p. 429–439.

Lal, D., and Peters, B., 1967, Cosmic ray produced radioactivity on the Earth, *in* Sitte, K., ed., Handbuch der Physik: Amsterdam, North Holland, v. 4612, p. 551–612.

Li Jijun, Derbyshire, E., and Xu Shuying, 1984, Glacial and paraglacial sediments of the Hunza Valley, north-west Karakoram, Pakistan: A preliminary analysis, *in* Miller, K., ed., International Karakoram Project: Cambridge, UK, Cambridge University Press, p. 496–535.

Lowe, J.J., and Walker, M.J.C., 1997, Quaternary environments: Harlow, UK, Longman, 446 p.

Martinson, D.G., Pisias, N.G., Hays, J.D., Imbrie, J., Moore, T.C., and Shackleton, N.J., 1987, Age dating and the orbital theory of the ice ages: Development of a high resolution 0–300,000-year chronostratigraphy: Quaternary Research, v. 27, p. 1–29.

Nishiizumi, K., Winterer, E.L., Kohl, C.P., Klein, J., Middleton, R., Lal, D., and Arnold, J.R., 1989, Cosmic ray production of ^{10}Be and ^{26}Al in quartz from glacially polished rocks: Journal of Geophysical Research, v. 94, p. 17907–17915.

Nishiizumi, K., Kohl, C.P., Arnold, J.R., Dorn, R., Klein, J., Fink, D., Middleton, R., and Lal, D., 1993, Role of in situ cosmogenic nuclides ^{10}Be and ^{26}Al in the study of diverse geomorphic processes: Earth Surface Processes and Landforms, v. 18, p. 407–425.

Nishiizumi, K., Finkel, R.C., Klein, J., and Hohl, C.P., 1996. Cosmogenic production of ^{7}Be and ^{10}Be in water targets: Journal of Geophysical Research, v. 101B, p. 22225–22232.

Owen, L.A., 1988, Terraces, uplift and climate in the Karakoram Mountains, northern Pakistan [Ph.D. thesis]: Leicester, UK, University of Leicester, 399 p.

Owen, L.A., 1989, Terraces, uplift and climate in the Karakoram Mountains, northern Pakistan: Karakoram intermontane basin evolution: Zeitschrift für Geomorphologie, N.F., v. 76, p. 117–146.

Owen, L.A., 1994, Glacial and nonglacial diamictons in the Karakoram Mountains and Western Himalayas, *in* Warren, W.P., and Croot, D.G., eds., Formation and deformation of glacial deposits: Rotterdam, Netherlands, A.A. Balkema, p. 9–28.

Owen, L.A., and Derbyshire, E., 1989, The Karakoram glacial depositional system: Zeitschrift für Geomorphologie, v. 76, p. 33–73.

Owen, L.A., and Derbyshire, E., 1993, Quaternary and Holocene intermontane basin sedimentation in the Karakoram Mountains, *in* Shroder, J.F., ed., Himalayas to the sea: Geology, geomorphology and the Quaternary: London, Routledge, p. 108–131.

Owen, L.A., Bailey, R.M., Rhodes, E.J., Mitchell, W.A., and Coxon, P., 1997, Style and timing of glaciation in the Lahul Himalaya, northern India: A framework for reconstructing late Quaternary palaeoclimatic change in the Western Himalayas: Journal of Quaternary Science, v. 12, p. 83–109.

Owen, L.A., Gualtieri, L., Finkel, R.C., Caffee, M.W., Benn, D.I., and Sharma, M.C., 2001, Cosmogenic radionuclide dating of glacial landforms in the Lahul Himalaya, northern India: Defining the timing of late Quaternary glaciation: Journal of the Quaternary Science, v. 16, p. 555–563.

Phillips, F.M., Zreda, M.G., Benson, L.V., Plummer, M.A., Elmore, D., and Sharma, P., 1996, Chronology for fluctuations in late Pleistocene Sierra Nevada glaciers and lakes: Science, v. 274, p. 749–751.

Phillips, W.M., Sloan, V.F., Shroder, J.F., Sharma, P., Clarke, M.L., and Rendell, H.M., 2000, Asynchronous glaciation at Nanga Parbat, northwestern Himalaya Mountains, Pakistan: Geology, v. 28, p. 431–434.

Pillewizer, W., 1957, Bewegungstudien an Karakorumgletschern: Gotha-Leipzig, Germany, VEB Hermann Haack Geographische-Kartographische Anstalt, Petermanns Geographische Mitteilungen Ergaenzungsheft 262, p. 53–60.

Prell, W.L., and Kutzbach, J.F., 1987, Monsoon variability over the past 150,000 yr: Journal of Geophysical Research, v. 92, p. 8411–8425.

Raymo, M.E., and Ruddiman, W.F., 1992, Tectonic forcing of late Cenozoic climate: Nature, v. 359, p. 117–122.

Richards, B.W.M., 2000, Luminescence dating of Quaternary sediments in the Himalaya and high Asia: A practical guide to the use and limitations for constraining the timing of glaciation: Quaternary International, v. 65/66, p. 49–61.

Richards, B.W., Owen, L.A., and Rhodes, E.J., 2000, Timing of late Quaternary glaciations in the Himalayas of northern Pakistan: Journal of Quaternary Science, v. 15, p. 283–297.

Richards, B.W., Benn, D.I., Owen, L.A., Rhodes, E.J., and Spencer, J.Q., 2001, Timing of late Quaternary glaciations south of Mount Everest in the Khumbu Himal, Nepal: Geological Society of America Bulletin, v. 112, p. 1621–1632.

Ruddiman, W.F., and Kutzbach, J.E., 1990, Late Cenozoic plateau uplift and climate change: Transactions of the Royal Society of Edinburgh: Earth Sciences, v. 81, p. 301–341.

Scott, C.H., 1992, Contemporary sediment transfer in Himalayan glacial systems [Ph.D. thesis]: Leicester, UK, University of Leicester, 352 p.

Searle, M.P., 1991, The geology and tectonics of the Karakoram Mountains: Chichester, UK, Wiley, 358 p.

Shackleton, N.J., Berger, A., and Peltier, W.R., 1990. An alternative astronomical calibration of the lower Pleistocene timescale based on ODP site 677: Transactions of the Royal Society of Edinburgh: Earth Science, v. 81, p. 251–261.

Sharma, M.C., and Owen, L.A., 1996, Quaternary glacial history of the Garhwal Himalaya, India: Quaternary Science Reviews, v. 15, p. 335–365.

Shi Yafeng, and Zhang Xiangsong, 1984, Some studies of the Batura glacier in the Karakoram Mountains, *in* Miller, K., ed., International Karakoram Project: Cambridge, UK, Cambridge University Press, p. 51–62.

Shroder, J.F., Khan, M.S., Lawrence, R.D., Madin, I.P., and Higgins, S.M., 1989, Quaternary glacial chronology and neotectonics in the Himalaya of northern Pakistan, *in* Malinconico, L.L., and Lillie, R.L., eds., Tectonics and Geophysics of the Western Himalaya: Geological Society of America Special Paper 232, p. 275–294.

Shroder, J.F., Owen, L.A., and Derbyshire, E., 1993, Quaternary glaciation of the Karakoram and Nanga Parbat Himalaya, *in* Shroder, J.F., ed., Himalaya to the sea: Geology, geomorphology and the Quaternary: London, Routledge, p. 132–158.

Sirocko, F., Sarnthein, M., Lango, H., and Erlenkeuser, H., 1991, The atmospheric summer circulation and coastal upwelling in the Arabian Sea during the Holocene and the last glaciation: Quaternary Research, v. 36, p. 72–73.

Sloan, V., Phillips, W.M., Shroder, J.F., Sharma, P., and Rendell, H., 1998, Asynchronous maximum advances of mountain glaciers in the Pakistan Himalaya: Geological Society of America Abstracts with Programs, v. 30, no. 7, p. A-229.

Small, E.E., Anderson, R.S., Repka, J.L., and Finkel, R., 1997, Erosion rates of alpine bedrock summit surfaces deduced from in situ Be-10 and Al-26: Earth and Planetary Science Letters, v. 150, p. 413–425.

Sternberg, R.S., 1996, Workshop on secular variation in the rate of production of cosmogenic nuclides on Earth: Paleomagnetic averages of geomagnetic latitude: Radiocarbon, v. 38, p. 169–170.

Stone, J.O., Allan, G.L., Fiefield, L.K., and Cresswell, R.G., 1996, Cosmogenic chlorine-36 from calcium spallation: Geochimica et Cosmochimica Acta, v. 60, p. 679–692.

Stone, J.O., Ballanyne, C.K., and Fifield, L.K., 1998a, Exposure dating and validation of periglacial weathering limits, northwest Scotland: Geology, v. 26, p. 587–590.

Stone, J.O., Evans, J.M., Allan, G.L., Fifield, L.K., and Cresswell, R.G., 1998b, Cosmogenic chlorine-36 production in calcite by muons: Geochimica et Cosmochimica Acta, v. 62, p. 433–454.

Taylor, P.J., and Mitchell, W.A., 2000, Late Quaternary glacial history of the Zanskar Range, north-west Indian Himalaya: Quaternary International, v. 65/66, p. 81–99.

Thompson, L.G., Thompson, E.M., Davies, M.E., Bolzn, J.F., Dai, J., Gunderstrup, N., Wu, X., Klein, L., and Xie, Z., 1989, Holocene–late Pleistocene climatic ice core records from the Qinghai-Tibet Plateau: Science, v. 246, p. 474–477.

Thompson, L.G., Yao, T., Davis, M.E., Henderson, K.A., Mosley-Thompson, E., Lin, P.-N., Beer, J., Synal, H.A., Cole-Dai, J., and Bolzan, J.F., 1997, Tropical climate instability: The last glacial cycle from a Qinghai-Tibetan ice core: Science, v. 276, p. 1821–1825.

MANUSCRIPT RECEIVED BY THE SOCIETY MARCH 7, 2001
REVISED MANUSCRIPT RECEIVED OCTOBER 15, 2001
MANUSCRIPT ACCEPTED NOVEMBER 19, 2001

Printed in the USA